AJNR

MR Imaging and Single-Photon Emission CT Findings after Gene Therapy for Human Glioblastoma

Frank W. Floeth, Albrecht Aulich, Karl J. Langen, Klaus J. Burger, Wolfgang J. Bock and Friedrich Weber

AJNR Am J Neuroradiol 2001, 22 (8) 1517-1527
http://www.ajnr.org/content/22/8/1517

AJNR Am J Neuroradiol 22:1517–1527, September 2001

MR Imaging and Single-Photon Emission CT Findings after Gene Therapy for Human Glioblastoma

Frank W. Floeth, Albrecht Aulich, Karl J. Langen, Klaus J. Burger, Wolfgang J. Bock, and Friedrich Weber

BACKGROUND AND PURPOSE: **Our goal was to evaluate MR imaging findings after local intracerebral gene therapy in patients with glioblastoma and differentiate postoperative contrast enhancement phenomena.**

METHODS: **In all, 26 patients with supratentorial single lesion glioblastoma underwent tumor resection and intracerebral injection of murine retroviral vector–producer cells for gene therapy with the herpes simplex virus type I thymidine kinase gene/ganciclovir system. Serial contrast-enhanced MR studies were obtained before treatment and postoperatively on day 1 or 2; weeks 2, 4, 9, 13, 17, 25, and 33; and every 8 weeks thereafter. Iodomethyltyrosine single-photon emission CT (IMT-SPECT) investigations also were performed in selected cases.**

RESULTS: **Twelve patients showed nontumorous enhancement of various intensities after treatment, arising within 18 to 72 hours and persisting at 3 to 10 months. It was characterized by a strong local enhancement up to 20 mm thick, which was initially nodular and later linear along the resection cavity wall and surrounded by massive perifocal edema. This "flare" enhancement had features that clearly differed from those of residual tumor enhancements and benign postsurgical enhancements. The IMT-SPECT investigations showed increased amino acid uptake in patients with enhancement from residual or relapsing tumor, but not in patients with flare.**

CONCLUSION: **After local gene therapy, a unique dynamic, transient perifocal flare enhancement can occur on MR images. IMT-SPECT may help to differentiate between tumorous and nontumorous flare enhancements in patients with enhancing tissue on MR images after gene therapy for glioblastoma.**

Glioblastomas are highly aggressive tumors, recurrent and fatal in 100% of cases and causing 12,000 deaths annually in the United States (1). Standard treatment consists of tumor debulking (2) followed by local irradiation (3). The median survival time after tumor resection and radiation for glioblastoma is 8 to 10 months (4) with local recurrence usually within 4 to 6 months (5). For relapsing disease, the life expectancy is restricted to less than 6 months (6).

The exceptional setting of malignant gliomas—rapidly proliferating tumors in a background of nondividing, functional neural tissue within the brain—makes them excellent candidates for selective, suicide gene transfer by a retroviral vector. Because retroviruses transfect only dividing cells, the therapy selectively affects tumor cells and spares neurons. The most common and best-investigated antitumor gene therapy strategy for glioma models is the herpes simplex virus type I thymidine kinase/ganciclovir (HSV-Tk/GCV) system. In this system, transfection of the tumor cells with the Tk gene, which is not present in human cells, causes them to produce the Tk enzyme. Nucleoside analogs such as GCV, which serve as prodrugs, are phosphorylated by the Tk to their active forms, which then lead to apoptotic cell death.

Measurement of therapeutic success after microsurgical tumor resection (with or without gene therapy), tumor recurrence, and progression of glioblastoma can be difficult. These outcomes are thought to relate directly to regression or progression of contrast enhancement on serial MR images. A major problem of postoperative imaging after glioma resection is the assessment of residual tumor. In postoperative MR imaging, the features of contrast enhancement within the operative field of-

Received May 22, 2000; accepted after revision April 13, 2001.

From the Departments of Neurosurgery (F.W.F., W.J.B., F.W.) and Diagnostic Radiology (A.A.), Heinrich-Heine-University, Düsseldorf; Institute of Medicine (K.J.L.), Research Center Jülich, Jülich; and Novartis Pharma GmbH (K.J.B.), Nürnberg, Germany.

This work was supported by Novartis Pharma GmbH, Nürnberg, Germany.

Address reprint requests to Frank Willie Floeth, MD, or Friedrich Weber, MD, Department of Neurosurgery, Heinrich-Heine-University of Düsseldorf, Moorenstrasse 5, 40225 Düsseldorf, Germany.

TABLE 1: Course and outcome of gene therapy treatments in 26 consecutive patients

Patient	Sex	Age (y)	Prior Therapy*	Surgery Date†	Enhancement (cm^3)‡	Flare§	Histologic Sample	Alive	Dead
1	M	37	S × 2, R	03/12/1996	8	++	⋯	57 mo	
2	F	70	S, R	04/03/1996	<1	−	⋯		13 mo
3	F	57	S, R	04/25/1996	3	+	Day 27		1 mo
4	F	40	S × 2, R	05/21/1996	16	−	⋯		9 mo
5	M	49	S, R	05/28/1996	<1	++	⋯		13 mo
6	M	60	S, R	05/30/1996	15	−	⋯		9 mo
7	M	50	S, R	06/05/1996	20	−	⋯		5 mo
8	M	36	S × 3, R	06/26/1996	22	−	⋯		5 mo
9	M	49	S, R	07/04/1996	<1	++	⋯		16 mo
10	M	54	S, R	07/28/1996	12	−	⋯		6 mo
11	F	68	⋯	01/15/1997	<1	−	⋯		4 mo
12	F	55	S, R	03/17/1997	8	+	Day 71		10 mo
13	F	72	⋯	05/12/1997	7	+	⋯		8 mo
14	F	60	⋯	05/22/1997	<1	−	⋯		6 mo
15	F	60	⋯	07/23/1997	7	−	Day 102		16 mo
16	M	68	⋯	09/04/1997	4	+	Day 183		14 mo
17	M	61	S, R	10/27/1997	4	−	Day 134		10 mo
18	M	58	⋯	12/18/1997	5	++	⋯		11 mo
19	M	67	⋯	01/15/1998	3	−	Day 145		12 mo
20	M	44	⋯	02/19/1998	14	++	Day 218		16 mo
21	M	38	⋯	02/24/1998	<1	++	⋯	34 mo	
22	M	66	S, R	02/26/1998	3	+	⋯		10 mo
23	F	82	⋯	03/26/1998	3	−	⋯		8 mo
24	F	67	⋯	03/31/1998	14	+	⋯		17 mo
25	M	60	S, R	05/07/1998	15	−	⋯		6 mo
26	M	58	S, R	09/17/1998	8	−	⋯		6 mo

* S, surgery; R, radiation therapy.

† Date of tumor resection and gene therapy.

‡ On MR images on day 1 or 2 postoperatively.

§ −, none; +, moderate; ++, strong.

ten are nonspecific; it may be impossible to differentiate tumorous enhancement from nontumorous, nonspecific postsurgical changes such as benign postsurgical enhancement.

In this study, we evaluated a unique form of enhancement occurring after tumor resection and local intracerebral gene therapy. In addition, we present two methods that may help to distinguish the different types of contrast enhancement phenomena after resection and gene therapy.

Methods

Between March 1996 and September 1998, 26 patients with progressive, supratentorial single-lesion glioblastoma (World Health Organization grade IV) were treated with gene therapy after tumor resection in three prospective, open-label clinical protocols approved by local ethics committees (Table 1).

Of the 26 patients, 15 with tumor relapse after previous surgery and radiation therapy had been enrolled into study GLIB 201-E, a Phase II, multicenter study of recurrent glioblastoma (patients 1–10) or study GTI 117, a Phase III, multicenter study of recurrent glioblastoma (patients 12, 17, 22, 25, and 26). All underwent repeat surgery followed by gene therapy. There were 21 patients with newly diagnosed and previously untreated tumors who had been enrolled into study GTI 115 (a Phase III, international, randomized study of primary glioblastoma), of which 10 had been assigned to the control group (surgery and standard radiation therapy [external beam partial-brain radiation with a cumulative dose of 30 × 2 Gy over 6 weeks, starting 2 to 3 weeks after surgery]), and 11 had been assigned to the treatment group (surgery, gene therapy, and standard radiation therapy; patients 11, 13–16, 18–21, 23, and 24). Thus, a total of 26 patients had received gene therapy, and 10 patients had served as control subjects.

After patients provided informed consent, they underwent surgery with representative biopsy sampling and maximal resection of the tumor. Only if the local neuropathologic analysis confirmed the intraoperative frozen-section diagnosis of vital glioblastoma did we administer gene therapy. We used murine vector-producer cell (VPC)-mediated HSV-Tk/GCV therapy.

The procedure comprises two phases: first, local application of the retroviral vector to transfect the tumor cells with the HSV-Tk suicide gene, and second, systemic administration of the prodrug GCV to induce death of the Tk-expressing cells. We injected mouse fibroblast VPC because they release high titers of the Tk-carrying vectors over 1 to 2 weeks. Compared with injection of vectors alone, treatment with VPC achieves much higher transduction rates. There are two approved strategies for the local application of the therapeutic: direct injection into the tissue during an open surgical procedure (the procedure we used) or external infusion by minipump (convection-enhanced delivery) after placement of an Ommaya catheter into the tumor.

The therapeutic agent used, GLI 328, was supplied by the Novartis affiliate, Genetic Therapy Inc. (Gaithersburg, MD, USA) (7, 8). GLI 328 is a retroviral VPC line containing the vector plasmid stably integrated into a packaging cell derived from mouse fibroblasts (9). Operative procedures and gene therapy delivery were strictly standardized in all patients. After a debulking procedure that aimed to resect the tumor completely, 9 to 10 mL of VPC (10^8 mouse fibroblasts/mL) were injected evenly into the infiltration zone of the surrounding white matter and into any residual tumor, in cases of subtotal

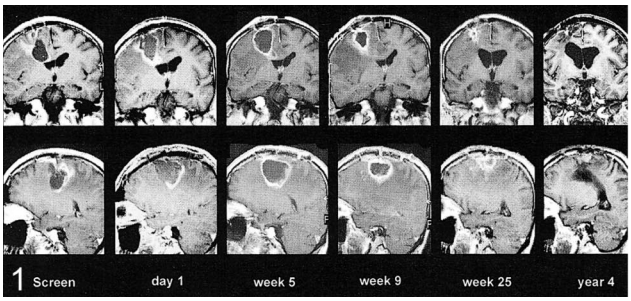

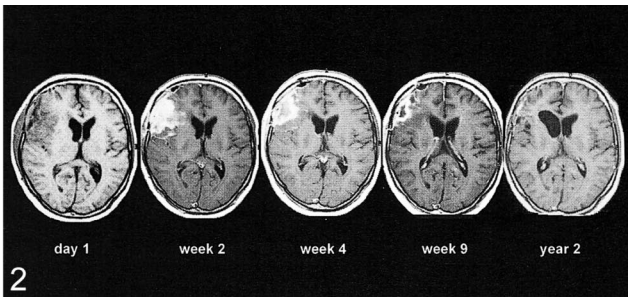

FIG 1. Flare enhancement. MR images obtained preoperatively and on day 1; weeks 5, 9, and 25; and year 4 postoperatively show development of a strong nodular flare very early with massive edema around the precentral resection cavity. Later images show progressive shrinking, leaving scarce residual evidence after 1 year (enhanced T1-weighted coronal and sagittal MR images, patient 1).

FIG 2. Flare enhancement. MR images obtained on day 1; weeks 2, 4, and 9; and year 2 after surgery. A strong flare develops after complete resection of all enhancing tissue within the frontal lobe. Later, there is shrinking and nearly complete disappearance of the process (enhanced T1-weighted axial MR images, patient 21).

resection (on day 0). The injections were given freehand with a blunt metal needle, about 3 to 10 mm apart, with a depth of 3 to 15 mm and 0.2-mL increments per injection, leading to about 45 to 50 single injections. Two weeks after surgery, patients began a 14-day period of intravenous GCV treatment (5 mg/kg twice daily).

All 26 gene therapy patients and the 10 control patients had enhanced MR scans immediately before surgery and postoperatively at least on day 1 or 2; at weeks 2, 4, 9, 13, 17, 25, and 33; and every 8 weeks thereafter. Volumetric data to quantify the enhancing tissue mass were calculated on the basis of the local Brainlab neuronavigation system. In 11 patients, postoperative single-photon emission CT (SPECT) also was performed after intravenous injection of 370–550 MBq 3-[^{123}I]iodo-α(-methyltyrosine (IMT). The method was the same as described previously (10). SPECT investigations were not part of the study protocols and therefore were obtained only in special cases of interest and at different time points.

Results

There were 10 women and 16 men enrolled who ranged in age from 36 to 82 years (average, 56.5 years) and in Karnofsky Performance Status from 60% to 100% (average of 82.5%) (Table 1).

MR Characteristics of Postoperative Contrast Enhancement

Benign, Perifocal Flare Enhancement after Complete Tumor Resection.—On the early postoperative MR images after complete tumor resection, a strong enhancement appeared locally around the resection cavity wall. This had a distribution pattern different from that of the preoperative enhancements. It arose usually within 24 to 48 hours after surgery and VPC injection, sometimes as early as 18 hours postoperatively. Initially, the enhancement distribution tended to be more nodular or irregular and surrounded by massive perifocal edema within the white matter. The whole process enlarged during the first postoperative weeks, gained a maximum thickness of 20 mm, and reached peak enhancement after 3 to 5 weeks. At that stage, the enhancement was more linear and evenly distributed around the resection cavity wall. Despite a moderate to severe mass effect, which sometimes caused midline shift and compression of the ventricles, this phenomenon never was clinically apparent, with no associated signs or symptoms. In the following months, the process was characterized by continuous shrinking of the resection cavity, regression of the edema, and slow vanishing of the enhancement within 1 year. Finally, it collapsed completely, leaving a small scar remnant (with no enhancement) as the only residual evidence of the previously large process. Figures 1 and 2 show examples of typical development of such pure ''flare'' enhancement without tumor relapse after complete tumor resection. Remarkable was the nodular enhancement, which later changed to a more-linear distribution associated with massive and long-lasting perifocal edema. Within 1 year, the process had stopped, with complete disappearance of all enhancement and ex vacuo enlargement of the ipsilateral ventricle. Figure 3 also shows development of a strong flare within 2 weeks after complete tumor resection and VPC-mediated gene therapy. In this case, there is normal regression of enhancement initially, but a later increase in enhancement because of tumor regrowth. This so-called flare phenomenon of transient, dynamic, local enhancement was evident in various intensity in 12 (46%) of 26 gene therapy patients.

The occurrence and intensity of flare enhancement was independent of tumor status and concurrent radiation therapy. Of 11 patients with previously untreated glioblastoma, all of whom underwent radiation therapy after gene therapy, six (55%) showed flare enhancement—three with strong flare and three with moderate flare, one of whom was a long-term survivor. Of 15 patients with recurrent glioblastoma, all of whom underwent radiation therapy before gene therapy, six (40%) developed flare enhancement—three with strong flare and three with moderate flare, one of whom was a long-term survivor.

Benign, Perifocal Flare Enhancement after Incomplete Tumor Resection.— In five patients, the early postoperative MR images showed clear evidence of residual tumor compared with the preop-

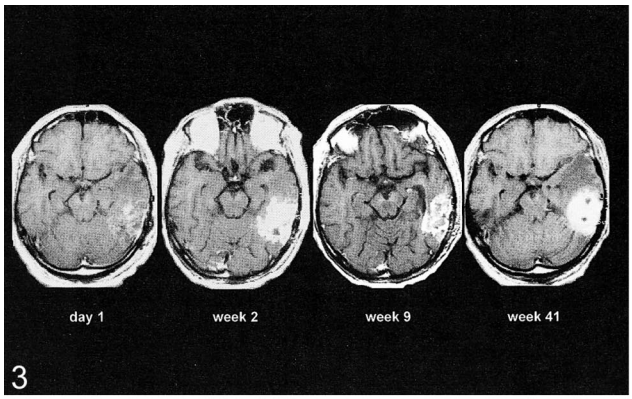

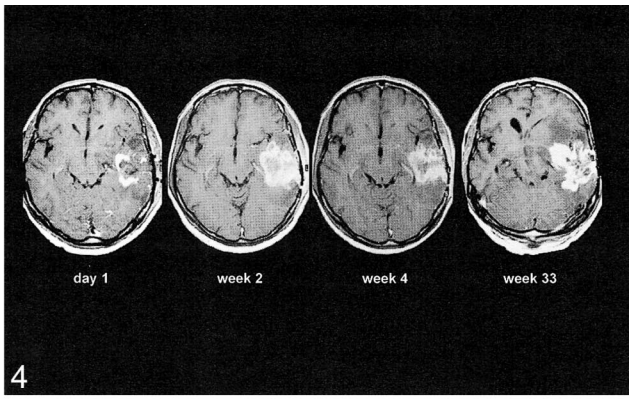

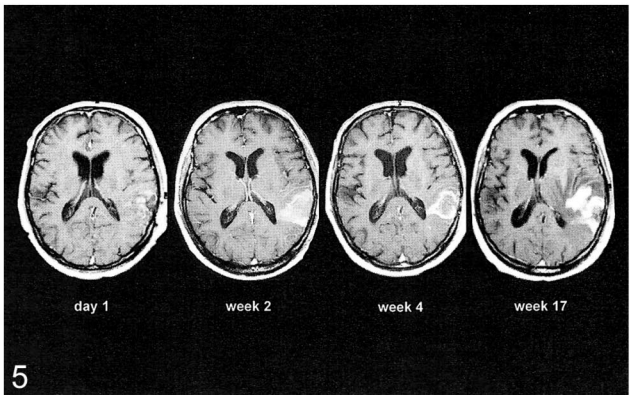

FIG 3. Flare enhancement and tumor relapse after complete resection. MR images obtained on day 1 and weeks 2, 9, and 41 postoperatively show development of a strong flare after resection of all enhancing tissue within the temporal lobe. There is initial regression of flare, but eventually there is recurrence of local tumor (enhanced T1-weighted axial MR images, patient 18).

FIG 4. Flare enhancement and tumor relapse after incomplete resection. MR images on day 1 and weeks 2, 4, and 33 after surgery show development of a strong flare after incomplete tumor resection with two remnants within the temporal lobe. The flare enhancement regresses at first, but eventually the tumor recurs from the remnants (enhanced T1-weighted axial MR images, patient 20).

FIG 5. Benign postsurgical enhancement. MR images from day 1 and weeks 2, 4, and 17 after tumor resection show development of thin, linear, benign enhancement and local tumor recurrence within the temporooccipital region (enhanced T1-weighted axial images, patient 19).

erative enhancement pattern, and later during follow-up, a strong flare was superimposed on the residual tumor enhancement. After the flare enhancement had regressed, residual tumor again was visible, reflecting relapse (Fig 4). This example is an excellent demonstration of the problem of interpreting postoperative enhancements without knowing when the image was obtained. It was easy to qualify the enhancement on day 1 as a tumor remnant, and it also was simple to decide at week 33 on a diagnosis of relapsing tumor. At weeks 2 and 4, however, it was impossible to differentiate the etiologic basis of the perifocal contrast enhancement within the old tumor bed.

Benign Postsurgical Enhancement.—Benign postsurgical enhancement was apparent in 11 patients (Fig 5), but not immediately after surgery. Within the weeks after surgery, MR images revealed a thin ring enhancement, only a few millimeters thick, with no surrounding edema or mass effect. Within the control group, seven of the 10 patients developed signs of benign postsurgical enhancement, but none of them showed MR imaging changes during follow-up similar to the above-described flare enhancement.

Outcomes of and Risk Factors for Flare Development.—The flare enhancement phenomenon was restricted to gene therapy patients, and its presence and intensity correlated with their outcomes (Table 1). In patients without flare (n = 14), tumor recurrence or progression of residual tumor developed early (average, within 2.2 months), and their survival ranged from 4 to 16 months (average, 8.2 months). Survival in patients with moderate flare (n = 6) ranged from 1 to 17 months (average, 10.0 months). Those with early and strong flare (n = 6) usually had a long relapse-free interval (average, 9.8 months) and a longer life expectancy (range, 11 to 57 months; average, 24.5 months), especially those without residual tumor. The two long-term survivors of the group both had very strong flare enhancement.

Of note, patients with flare were younger than those without flare (average, 55 versus 59 years, respectively), had smaller residual tumors (5.8 versus 9.1 cm^3), and more often had primary tumors

TABLE 2: Enhancing tissue volumes (cm^3) before and after gene therapy

		After Therapy													
			Week									Year			
Patient	Before Therapy	Day 1 or 2	2	4	9	13	17	25	33	41	49	1	2	3	4
1	28*	8	28	31	22*	18	12	8*	5	5	3	<1*	<1*	<1*	<1*
2	22	<1	5	7	6	5	11	26	…	…	…	†			
3	43	3	17	†											
4	56	16	18	21	25	42	…	…	…	†					
5	38	<1	11	22	18	13	28	…	…	…	…	†			
6	35	15	17	19	23	26	33*	45	…	†					
7	45	20	21	24	32	43	…	†							
8	42	22	23	23	34	48	…	†							
9	35	<1	3	10	16	18	12	…	…	…	…	…	†		
10	46	12	12	14	25	29	…	†							
11	10	<1	4	7	8	…	†								
12	30*	8	19	11*	18	§	12	22	†						
13	46	7	17	28	31	45	41	28	†						
14	18	<1	6	7	21	20	28	†							
15	12	7	9	7	8	11*	13	§	<1	<1	8	12	†		
16	41	4	6	10	13	29	21	25	§	8	23	…	†		
17	22*	4	6	7	15	16	28	§	23	†					
18	43	5	24	26*	19	17*	15	11	20	48	†				
19	12*	3	8	9*	9	13*	29*	§	23	28	38	§	†		
20	57	14	30*	32	26*	22	21	53	§	26	31	78	†		
21	46	<1	17	23*	19*	14	9	8	4	5	2	2	<1*	§	
22	25*	3	18	19*	10	12	23	35	…	…	†				
23	7	3	5	8*	7	15	…	…	…	†					
24	27	14	33	30*	31	27	21	20	41	53	§	28	†		
25	68	15	17	22	28	34	45	†							
26	39*	8	11	15	25	…	…	†							

* IMT-SPECT also obtained.

† Patient died.

§ Surgery performed.

(50% versus 36%). Factors such as age, general state of health, tumor location, primary versus recurrent disease, and tumor volume are of great relevance to prognosis. The mean survival times (MST) of our group confirmed these observations: being younger (<60 years old; n = 13; MST, 14.5 months), having a newly diagnosed glioblastoma (n = 11; MST, 13.2 months), and showing little to no residual tumor after surgical resection (<6 cm^3; n = 14; MST, 14.9 months) all predicted a better outcome. In contrast, older patients (≥60 years old; n = 13; MST, 10.2 months), those with recurrent glioblastoma (n = 15; MST, 11.7 months), and those with a large tumor remnant after surgery (≥6 cm^3; n = 12; MST, 11.7 months) had less favorable prognoses.

According to these observations, the patients with flare enhancement had a better constellation of prognostic factors, which could partly explain their better outcome. The number of patients was too small, however, to allow multivariate analysis of the prognostic significance of a certain factor.

Volumetric Characteristics of Postoperative Contrast Enhancement

We conducted volumetric evaluations of enhancing tissue and generated enhancement-volume curves for the complete time course of the patients after treatment (Table 2).

Flare Enhancement.—Figure 6 shows the graphical features of enhancement volumetry in postoperative flare enhancement. The typical flare phenomenon was characterized by a rapid increase in enhancement volume within the first 2 weeks after surgery, to up to 17–30 cm^3. After 3 to 5 weeks, the enhancement volume peaked at between 23 and 32 cm^3. Within the following weeks, the flare showed a slow, but continuous, linear decrease.

In patients with complete initial tumor resection and no recurrence, flare enhancement disappeared completely within 1 year (patients 1 and 21), and the curve resembled an asymmetrical mountain. In patients with incomplete tumor resection (patient 20) or relapse (patient 18), the regression of flare enhancement eventually was overcome by the increasing volume of the expanding tumor enhancement.

Residual Tumor Enhancement and Benign Postsurgical Enhancement.—Figure 7 illustrates the graphical features of follow-up enhancement volumetry in patients with residual tumor enhancement after incomplete tumor resection and in benign postsurgical enhancement after radical tumor resection.

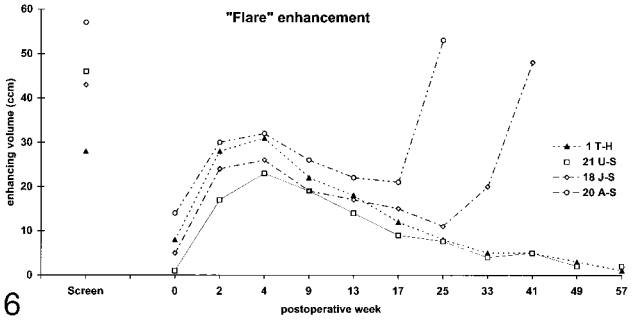

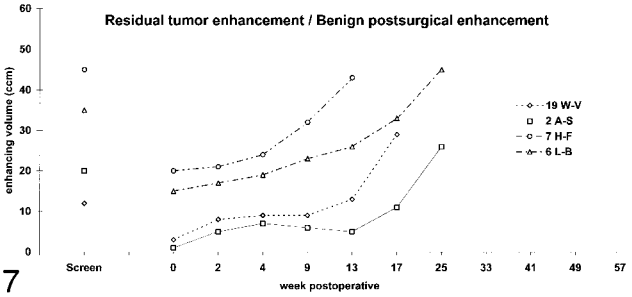

FIG 6. Volume curves of enhancing tissue during the postoperative course of four patients with flare. There is an early and quick increase in enhancement volume, a high peak at 4 weeks, and slow but continuous decrease during the following months. In patients without tumor recurrence, flare enhancement disappears within 1 year (patients 1 [*triangles*] and 22 [*squares*]). In case of tumor recurrence, the regression of flare enhancement is overcome by increasing tumor enhancement (patients 18 [*diamonds*] and 20 [*circles*]). The ''Screen'' point at the bar reflects the preoperative volume of enhancing tumor. For presentation, data for the postoperative images on day 1 or 2 are fixed to week 0, and note the nonlinear time axis.

FIG 7. Volume curves of benign postsurgical enhancement and residual tumor in two patients with benign postsurgical enhancement and two patients with residual tumor. For benign postsurgical enhancement, there is a delayed and slow increase in enhancement volume, stabilization at a plateau (instead of reaching a peak), and no significant regression. In the later course, the curve is moving upward because of recurrent tumor enhancement (lower two curves; patients 2 [*squares*] and 19 [*diamonds*]). Patients with residual tumor without flare or benign postsurgical enhancement show a continuous increase in enhancement volume because of tumor progression (upper two curves; patients 6 [*triangles*] and 7 [*circles*]). The ''Screen'' point at the bar reflects the preoperative enhancing tumor volume. For presentation, data for the postoperative images on day 1 or 2 are fixed to week 0, and note the nonlinear time axis.

Residual tumor was characterized by considerable contrast enhancement on early postoperative images. This was followed by a continuous increase in the volume of enhancement, linear during the first weeks and rising rapidly afterward (patients 6 and 7). The features of benign postsurgical enhancement included an initial absence of enhancement followed by a slow increase in enhancement volume to <10 cm^3 over the first weeks. The enhancement curve had no discernible peak and appeared to reach a plateau. After a temporary stabilization, the enhancement volume then increased rapidly later during follow-up because of regrowing tumor (patients 2 and 19).

IMT-SPECT Characteristics of Postoperative Contrast Enhancement

By comparing the volume of contrast enhancement on MR images with the amino acid uptake behavior on the SPECT scans, we addressed whether IMT-SPECT could differentiate the different kinds of postoperative enhancement on MR images (Table 2).

In two patients with complete tumor resection and early flare enhancement on the postoperative MR image (patients 1 and 18), the simultaneously obtained IMT-SPECT scan showed no increase in amino acid uptake. Further follow-up showed regression of enhancement and either no or late tumor relapse. Figure 8 shows the contrast enhancement on MR images and the amino acid uptake on IMT-SPECT scans during the pre- and postoperative course in patient 1. Preoperatively, the enhancement on MR images corresponded with an increased, circumscribed area of amino acid uptake on SPECT scans, indicating tumor. Immediately after surgery, the distribution of enhancement on MR images was completely different from that of the preoperative image, supporting that the new enhancement did not reflect tumor enhancement. At postoperative week 9, the MR image revealed a thick, ring-shaped, perifocal enhancement but the SPECT scan showed no increase in amino acid uptake, indicating that the enhancement on the MR image was nontumorous. This assumption was supported by later follow-up; at 1 year, the enhancement had vanished completely from MR images and the SPECT scans remained unremarkable.

One patient with a typical flare enhancement pattern and complete regression of all enhancement after 2 years showed an area of increased amino acid uptake on SPECT scans unchanged over the entire follow-up period (patient 21; scan not shown). After 28 months, he had clinical deterioration and showed increased enhancement on MR images. He underwent repeat surgery for extensive local tumor relapse.

In eight patients with postoperative enhancement on MR images and suspicion for residual or recurrent tumor, the simultaneously obtained SPECT scans were positive with hot-spot uptake of IMT (patients 6, 12, 15, 19, 20, 22, 23, 24). The follow-up MR images confirmed immediate tumor progress in all eight cases.

Figure 9 shows the images of a patient with suspected residual tumor after resection of a large, strongly enhancing temporal tumor (patient 20). One day after surgery, there were two small enhancing lesions at the medial aspect of the operative field. Compared with the enhancement distribution of tumor on the preoperative images, these lesions most likely were tumor remnants, but an early nodular flare also was possible. Follow-up images showed development of a strong, circular flare enhancement that completely integrated the

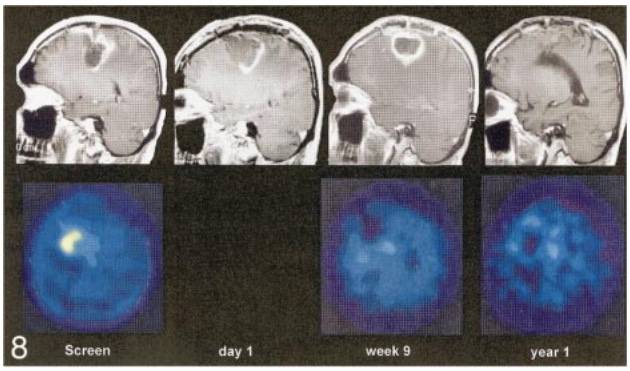

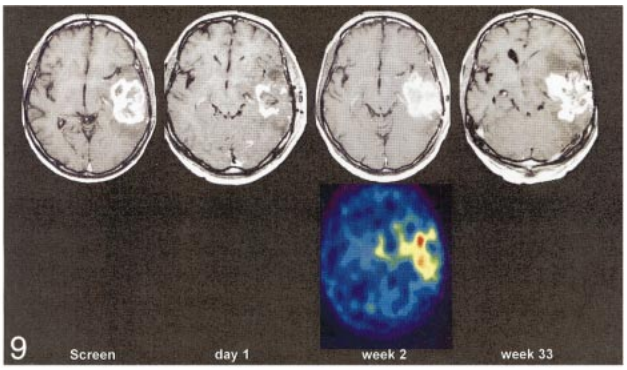

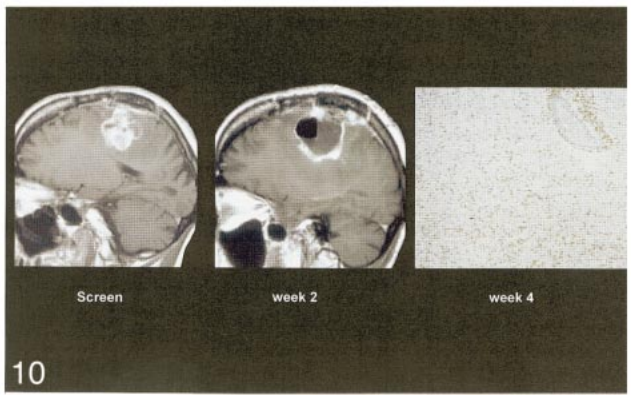

FIG 8. Flare enhancement at IMT-SPECT. Scans obtained preoperatively and on day 1, week 9, and year 1 postoperatively show enhancement on MR images (*upper line*) and amino acid uptake on IMT-SPECT scans (*lower line*). Although preoperative tumor enhancement on MR images corresponds with an increased amino acid uptake on SPECT scans, the postoperative flare on MR images shows no raised amino acid uptake on SPECT scans (enhanced T1-weighted sagittal MR images and IMT-SPECT scans, patient 1).

FIG 9. Flare enhancement and residual tumor at IMT-SPECT. Images obtained on day 1 and weeks 2 and 33 postoperatively show enhancement on MR images (*upper line*) and amino acid uptake on IMT-SPECT scans (*lower line*). The preoperative MR image shows a large, temporal, enhancing tumor mass. On day 1, two enhancing lesions are visible, which are completely incorporated into a strong flare enhancement at week 2. Tumor enhancement and flare enhancement are indistinguishable on MR images. The SPECT scan at week 2 reveals two ''hot'' spots of amino acid uptake corresponding to the two tumor remnants visible on MR images at day 1. By week 33, a nodular tumor recurrence has developed from the area of the two tumor remnants (enhanced T1-weighted axial MR images and IMT-SPECT scans, patient 20).

FIG 10. Flare enhancement and histologic findings. Preoperative MR image shows a large, precentral tumor relapse. At 2 weeks after complete resection, a moderate flare enhancement has developed at the margin of the large resection cavity. At week 4, multiple biopsies from the resection cavity wall (obtained at autopsy) show strong infiltration by inflammatory cells (tissue-resident macrophages and strong perivascular cuffs of lymphocytes) but no tumor (contrast-enhanced T1-weighted sagittal MR images; CD-68 immunostaining, magnetization $\times$ 20; patient 3).

two medial lesions. This made the individual lesions invisible and an etiologic interpretation impossible. The simultaneous SPECT scan revealed two distinct hot spots medially that corresponded to the two enhancing spots on the early postoperative MR image, indicating that they were tumorous. Follow-up confirmed this assumption; the patient had a local relapse of tumor arising from the two medial remnants.

Histologic Findings

Histologic specimens were obtained from seven patients at different intervals after treatment: days 27, 71, 102, 134, 145, 183, and 218. The earliest specimen (day 27) was obtained at autopsy from patient 4, after a fatal pulmonary embolism had occurred; all others were obtained during repeat operations for tumor relapse (Table 1). The tissue was not taken as a small-needle biopsy and not excised from the field of the recurrent tumor. For etiologic investigation of the flare phenomenon, multiple representative histologic samples were collected from the resection cavity wall and the adjacent white matter. The striking finding for the early specimens (days 27, 71, and 102) was strong infiltration of the resection cavity wall with inflammatory cells (Fig 10). There was a combination of diffuse, very intense macrophage infiltration and perivascular lymphocytic cuffs in otherwise healthy-appearing white matter. In the later specimens (days 134, 145, 183, and 218), the macrophage infiltration typically had vanished and only dense perivascular lymphocytic networks were apparent.

Discussion

To our knowledge, this is the largest single-center experience with MR imaging, and the only pre-

sentation of concomitant IMT-SPECT data, in VPC-mediated gene therapy. After local gene therapy, we noted a new type of dynamic, transient perifocal (flare) enhancement on MR images in certain patients. The IMT-SPECT investigations showed increased amino acid uptake in patients with enhancement from residual or relapsing tumor, but not in patients with flare. Thus IMT-SPECT may help to differentiate between tumorous and nontumorous flare enhancements in patients with enhancing tissue on MR images after gene therapy for glioblastoma.

The presence or absence of contrast enhancement within the suspected area of glioblastoma is thought to be a direct reflection of initial tumor size and the spread and development of tumor recurrence. The diagnostic value of contrast enhancement after surgical interventions, such as tumor resection, can become confusing. In these situations, enhancement may reflect residual tumor or it may reflect nonspecific enhancing phenomena such as inflammatory reactions or posttraumatic (postsurgical) tissue changes.

The so-called benign postsurgical enhancement is known to arise at the resection margins after surgical interventions such as tumor extirpations. Its characteristics include an absence of enhancement for the first 72 hours; development of a linear, thin enhancement at the edges of the resection cavity by the end of the first postoperative week; and persistence of the enhancement for a maximum of 3 months. It usually is not surrounded by substantial edema and does not cause mass shift. Potential underlying mechanisms include disruption of local blood-brain barrier, neovascularization, and luxury perfusion. Although residual tumor enhancement generally appears more nodular and irregular, postsurgical enhancement usually is linear. Knowledge of this phenomenon led to the recommendation that postoperative control images be obtained as early as possible after an operation, to distinguish between tumorous and nontumorous postsurgical enhancements (5). The reference standard for postoperative evaluation of residual tumor is thought to be an MR image within 48 hours after the procedure.

Benign postsurgical enhancement is not restricted to tumor surgery patients, however. It occurs after many different cerebral surgical procedures. In exceptional cases, benign enhancement can arise as early as 17 hours after nontumor surgery (such as temporal lobectomy for epilepsy) and it can appear to be both linear and nodular (11). This highlights that differentiation of contrast enhancement on postoperative MR images can be very difficult and that the presence of early postoperative enhancement alone does not always mean a diagnosis of residual neoplasm.

With the introduction of local intracerebral and intratumoral immunotherapies and gene therapy strategies, a pattern of nontumorous, transient posttreatment enhancement, termed ''flare'', was described. Smith et al (12) reported a strong flare enhancement on follow-up MR scans after intralesional immunotherapy for recurrent high-grade astrocytoma. Treatment consisted of radical tumor resection, placement of an Ommaya catheter in the surgical bed, and infusion of autologous tumor-infiltrating lymphocytes and interleukin-2. Immediately after therapy, four of six patients showed a flare phenomenon characterized by increased nodular enhancement, increased edema, and mass effect. Three months later, these findings had resolved completely. Three patients who showed flare enhancement after radical tumor extirpation remained tumor-free for 1 year. All three patients with incomplete tumor resection (one with and two without flare) had early tumor progression. The authors concluded that the flare phenomenon reflects an inflammatory immune response with favorable prognostic implications, especially after radical resection of the enhancing tumor bulk, that should disappear within 3 months. Persistent enhancement should be regarded as highly suspicious for tumor relapse. The authors mention that the differentiation of residual or recurrent tumor and flare enhancement can be difficult because of their similar features.

Deliganis et al (13) published the results of serial MR imaging in patients receiving gene therapy for recurrent glioblastoma. A series of seven patients received at least two cycles of VPC injection after gross total tumor resection and Ommaya catheter implantation. Three patients showed the typical features of flare—an early increase of enhancing tissue volume within 5 to 10 weeks after surgery, followed by a decrease or a plateau in enhancement. One patient had a stable postoperative enhancement volume for 19 weeks, and the remaining three patients had a continuous increase in enhancing tissue volume.

The flare enhancement in VPC-mediated gene therapy was shown to reflect an immune reaction to the injection of the xenogenic mouse fibroblasts, as a part of the ''bystander effect'' of the therapy. That a local inflammatory response of the host was the histopathologic mechanism for the enhancing phenomena was confirmed by immunohistochemical studies. Biopsy specimens collected from the enhancing areas showed strong infiltration of the white matter by cytokines, macrophages, and tumor-infiltrating T-lymphocytes (14, 15).

Our results showed flare phenomena—the increasing linear and nodular perifocal enhancement, increasing edema, and mass effect—similar to those described by others. Compared with the enhancement phenomena described above, however, the flare after multiple injections of VPC was stronger and lasted longer in the current study. The multiple injections of xenogenic mouse fibroblast VPCs deep into the white matter likely induced traumatic disruption of the local blood-brain barrier with subsequent migration of immune cells into this tissue. The combined effect of the initially

traumatic and later immunologic lesions of the blood-brain barrier likely led to the strong contrast uptake, which appeared as perifocal, transient, and self-limiting flare enhancement. Nearly 50% of the 26 patients in the treatment group, who had undergone tumor resection and local gene therapy, developed flare enhancement of different intensity. In contrast, none of the 10 patients of the control group, who had undergone tumor resection alone, showed any features similar to flare. Similar to the results described by Smith et al (12), the patients who expressed flare signs had a favorable prognosis, especially those with radical tumor resection and strong flare. This latter group showed recurrence-free periods of up to 4 years. It is unclear why, despite highly standardized treatment, some patients exhibited flare enhancement reactions and some did not.

The morphologic feature of contrast enhancement within the operative field on CT scans or MR images has poor diagnostic specificity (16), and on MR images, flare can be indistinguishable from residual tumor after incomplete resection. In our study, flare immediately after surgery had a nodular and irregular shape, with a thickness of up to 20 mm, resembling that of residual tumor. In later follow-up, it usually formed a linear, ring-shaped enhancement around the resection cavity with perifocal edema and signs of mass shift, resembling tumor recurrence. Astonishingly, even strong flare, with massive edema, consecutive midline shift, and compression of the ventricles, was completely inapparent clinically. The patients showed no symptoms of increased intracranial pressure, such as headaches, nausea, visual disturbances, or focal neurologic deficits, and they were not dependent on steroid treatment for edema. This is somewhat atypical of enhancement from tumor recurrence, which usually is connected with clinical deterioration and the need for steroid treatment.

The situation of an unclear postoperative local enhancement is unsatisfactory for both the patient and the clinician. A reliable differentiation of tumorous from nontumorous enhancement is crucial for further treatment planning. With an incorrect interpretation, surgical interventions and medical treatment might be performed unnecessarily or delayed. There are two strategies to rule out residual or recurrent tumor: 1) obtaining follow-up MR images to observe the natural course of the morphologic appearance of the suspect enhancement, and 2) gather additional information about the metabolic activity of the enhancing lesion through positron-emission tomography (PET), SPECT, or MR spectroscopic (MRS) investigations.

On follow-up MR images in the current study, the dynamic changes in enhancement volume appeared to be specific for the different entities: 1) Flare was characterized by a very early and explosive increase in enhancement volume, with a peak after 1 month and slow regression over 1 year, and the enhancement-volume curve over time resembled a mountain; 2) benign postsurgical enhancement appeared later and showed a slow increase of enhancement volume over the first postoperative weeks with no real peak, and the volume curve resembled a flat hill; and 3) residual tumor or early tumor recurrence showed slow but continuous rise in enhancement early during follow-up, followed by an explosive increase in the enhancement volume.

This simple follow-up strategy has several disadvantages and hazards, however. For example, in the interim, the patient has to withstand the uncertainty that tumor relapse might not be diagnosed in time to adjust the therapy regimen. The control image also might show an advanced tumor relapse. Furthermore, a single follow-up scan might not be specific enough, such that further control images would need to be obtained.

Our examples show that the interpretation of postoperative enhancement depends greatly on the timing of the follow-up image. The reference standard for performing postoperative MR imaging is within 48 hours after the procedure, which should avoid the appearance of secondary and nonspecific enhancing tissue changes (5). However, this standard is unreliable in cases of flare enhancement after local gene therapy. The shape of postoperative enhancement also is nonspecific. It is thought that nodular enhancement most likely represents residual tumor, whereas linear enhancement indicates secondary, nontumorous enhancement. We have shown that massive flare enhancement can arise within 24 hours of surgery and be both nodular and linear in shape. Furthermore, a massive flare can be superimposed over tumor remnants and ''hide'' them for several months. Thus, the simple follow-up strategy cannot be recommended in every case.

The second strategy, metabolic investigation, offers an opportunity for noninvasive monitoring of the biology and metabolic activities of a lesion. It also has the potential to give reliable information, such as whether a suspect enhancement reflects vital neoplastic tissue, in a single investigation with no waiting period. A typical feature of glioma, especially the rapidly proliferating glioblastoma, is a hypermetabolic state. Compared with nonneoplastic enhancing lesions, such as radiation necrosis, benign postsurgical enhancement, or inflammatory changes, vital high-grade glioma tissue usually is characterized by an increased uptake of glucose or amino acids with typical hot-spot formation on PET and SPECT scans (17–22). MRS and MRS imaging can provide an overview of the concentrations of defined metabolites within the brain and differentiate neoplastic lesions from other tissue effects. Vital glioblastoma tissue usually shows a specific constellation of metabolic variables: high concentration of choline metabolites and glycine, reduced concentration or absence of creatine metabolites, absence of *N*-acetylaspartate, presence of lipid signals, and variable concentration of lactate. Because of the extensive inter- and intraindividual

heterogeneity of high-grade gliomas, metabolite concentrations have varied considerably in vivo and in vitro (23–32).

In cases of unclear enhancing tissue, alternative metabolic investigations such as PET, which uses ^{18}F-deoxyglucose or radiolabeled amino acids, and MRS can differentiate tumorous from nontumorous lesions. We used IMT-SPECT in this study, which is routinely available in our department. This method was able to differentiate tumorous from nontumorous enhancement phenomena as well as PET can, with a single investigation. Although the unnatural amino acid IMT is not incorporated into protein (33), the results of this method in cerebral gliomas are similar to those of PET investigations using ^{11}C-L-methionine (10). This is because transport is the dominant mechanism for the increased uptake of amino acids in cerebral gliomas. Initial clinical investigations have shown that IMT is well suited to differentiate cerebral gliomas from benign lesions (34). Inflammatory lesions showed only low IMT uptake.

In our study, preoperative tumor, postoperative residual tumor, and tumor recurrences were detected safely by a circumscribed hot-spot formation or locally increased uptake at IMT-SPECT. Even small tumor remnants, which were completely integrated into a strong flare enhancement, were detected. In cases of pure flare, SPECT usually did not show increased IMT uptake after gene therapy. The only patient with flare enhancement, who had continuous hot-spot formation at IMT-SPECT despite complete regression of enhancement after 2 years, had tumor relapse with increasing enhancement after 28 months.

The intensity of IMT uptake and hot-spot formation did not correlate with the extension and intensity of contrast enhancement on MR images. This is in agreement with observations that IMT uptake is independent from contrast enhancement on CT scans or MR images (10) and sometimes can show tumor infiltration that is not visible even on standard T2-weighted MR studies (35). Like other metabolic investigations, IMT-SPECT clearly can provide valid, qualitative information about the presence or absence of tumorous tissue in a single investigation. It appears to be a promising alternative to PET or MRS in cases of unclear enhancement phenomena suspicious for tumor. Unfortunately, we did not obtain IMT-SPECT scans routinely in all patients during the entire follow-up period, thus we can rely on only a limited number of well-documented cases.

Conclusion

After resection and gene therapy (multiple injections of mouse fibroblast VPC) for human glioblastoma, a unique type of nontumorous, transient flare enhancement can be detected along the resection cavity wall. It is characterized by its appearance within 1 to 3 days after surgery, a nodular or linear shape, and a dramatic increase in enhancement with a peak at 1 month. This flare, which can reach a maximum thickness of 20 mm and is surrounded by a strong perifocal edema, regresses slowly within 1 year. The histopathologic basis most likely is a combination of injection-induced trauma and xenogenic rejection activity, which induces local inflammation and disruption of the blood-brain barrier with subsequent infiltration by immune cells. This leads to perifocal contrast leakage, visible as strong flare enhancement. Clinically, the patients are unremarkable, showing no signs or symptoms despite the edema and mass shift. Particularly after radical tumor resection, a strong flare reaction seems to predict a better prognosis.

On MR imaging, nontumorous enhancement phenomena such as flare or benign postsurgical enhancement can be indistinguishable from enhancement from residual or relapsing tumor. Metabolic investigation with IMT-SPECT seems to offer an immediate and reliable method to rule out neoplastic tissue in cases of unclear contrast enhancement. In our patients, vital glioblastoma tissue consistently showed a circumscribed hot spot of amino acid uptake, whereas flare showed no increased IMT uptake at SPECT. Like PET and MRS, metabolic imaging with IMT-SPECT appears to be a reliable method to differentiate unclear MR contrast enhancement phenomena after local gene therapy.

References

1. Davis FG, Malinski N, Haenszel W, et al. **Primary brain tumor incidence rates in four United States regions, 1985–1989: a pilot study.** *Neuroepidemiology* 1996;15:103–112
2. Devaux BC, OFallon JR, Kelly PJ. **Resection, biopsy and survival in malignant glial neoplasms.** *J Neurosurg* 1993;78: 767–775
3. Sheline GE. **Radiotherapy for high-grade gliomas.** *Int J Radiat Oncol Biol Phys* 1990;18:793–803
4. Kiwit JCW, Floeth FW, Bock WJ. **Survival in malignant glioma: analysis of prognostic factors with special regard to cytoreductive surgery.** *Zentralbl Neurochir* 1996;57:76–88
5. Albert FK, Forsting M, Sartor K, Adams HP, Kunze S. **Early postoperative magnetic resonance imaging after resection of malignant glioma: objective evaluation of residual tumor and its influence on regrowth and prognosis.** *Neurosurgery* 1994;34: 45–61
6. Rajan B, Ross G, Lim CC, et al. **Survival in patients with recurrent glioma as a measure of treatment efficacy: prognostic factors following nitrosourea chemotherapy.** *Eur J Cancer* 1994;30A:1809–1815
7. Long Z, Lu P, Grooms T, et al. **Molecular evaluation of biopsy and autopsy specimens from patients receiving in vivo retroviral gene therapy.** *Hum Gene Ther* 1999;10:733–740
8. Shand N, Weber F, Mariani L, et al. **A Phase 1–2 clinical trial of gene therapy for recurrent glioblastoma multiforme by tumor transduction with the herpes simplex thymidine kinase gene followed by ganciclovir.** *Hum Gene Ther* 1999;10: 2325–2335
9. Miller AD, Buttimore C. **Redesign of retrovirus packaging cell lines to avoid recombination leading to helper virus production.** *Mol Cell Biol* 1986;6:2895–2902
10. Langen K-J, Ziemons K, Kiwit JCW, et al. **[^{123}I]Iodo-α-methyltyrosine SPECT and [^{11}C]-L-methionine uptake in cerebral gliomas: a comparative study using SPECT and PET.** *J Nucl Med* 1997;38:517–522

11. Henegar MM, Moran CJ, Silbergeld DL. **Early postoperative magnetic resonance imaging following nonneoplastic cortical resection.** *J Neurosurg* 1996;84:174–179
12. Smith MM, Thompson JE, Castillo M, et al. **MR of recurrent high-grade astrocytomas after intralesional immunotherapy.** *AJNR Am J Neuroradiol* 1996;17:1065–1071
13. Deliganis AV, Baxter AB, Berger MS, Marcus SG, Maravilla KR. **Serial MR in gene therapy for recurrent glioblastoma: initial experience and work in progress.** *AJNR Am J Neuroradiol* 1997; 18:1401–1406
14. Ram Z, Culver KW, Oshiro EM, et al. **Therapy of malignant brain tumors by intratumoral implantation of retroviral vector-producing cells.** *Nature Med* 1997;3:1354–1361
15. Ramesh R, Marrogi AJ, Freeman SM. **Tumor killing using the HSV-tk suicide gene.** *Gene Ther Mol Biol* 1998;1:253–263
16. Zimmerman RA. **Imaging of adult central nervous system primary malignant gliomas. Staging and follow up.** *Cancer* 1991; 67:1278–1283
17. Barker FG II, Chang SM, Valk PE, et al. **18-Fluorodeoxyglucose uptake and survival of patients with suspected recurrent malignant glioma.** *Cancer* 1997;79:115–126
18. Fulham MJ, Di Chiro G. **Neurologic PET and SPECT.** In: Harbert T, Eckelman W, Neumann R, eds. *Textbook of Nuclear Medicine.* Basel: Thieme; 1996;361–385
19. Davis WK, Boyko OB, Hoffman JM, et al. **[^{18}F]2-fluoro-2-deoxyglucose-positron emission tomography correlation of gadolinium-enhanced MR imaging of central nervous system neoplasia.** *AJNR Am J Neuroradiol* 1993;14:515–523
20. Herholz K, Pietrzyk U, Voges J, et al. **Correlation of glucose consumption and tumor cell density in astrocytomas. A stereotactic PET study.** *J Neurosurg* 1993;79:853–858
21. Schifter T, Hoffman JM, Hanson MW, et al. **Serial FDG-PET studies in the prediction of survival in patients with primary brain tumors.** *J Comput Assist Tomogr* 1993;17:509–516
22. Kim CK, Alavi JB, Alavi A, et al. **New grading system of cerebral gliomas using positron emission tomography with F-18 fluorodeoxyglucose.** *J Neurooncol* 1991;10:85–91
23. Kaibara T, Tyson RL, Sutherland GR. **Human cerebral neoplasms studied using MR spectroscopy: a review.** *Biochem Cell Biol* 1998;76:477–486
24. Preul MC, Leblanc R, Caramanos Z, et al. **Magnetic resonance spectroscopy guided brain tumor resection: differentiation between recurrent glioma and radiation change in two diagnostically difficult cases.** *Can J Neurol Sci* 1998;25:13–22
25. Tedeschi G, Lundbom N, Raman R, et al. **Increased choline signal coinciding with malignant degeneration of cerebral gliomas: a serial proton magnetic resonance spectroscopy imaging study.** *J Neurosurg* 1997;87:516–524
26. Kinoshita Y, Yokota A. **Absolute concentrations of metabolites in human brain tumors using in vitro proton magnetic resonance spectroscopy.** *NMR Biomed* 1997;10:2–12
27. Shimizu H, Kumabe T, Tominaga T, et al. **Noninvasive evaluation of malignancy of brain tumors with proton MR spectroscopy.** *AJNR Am J Neuroradiol* 1996;17:737–747
28. Preul MC, Caramanos Z, Collins DL, et al. **Accurate, noninvasive diagnosis of human brain tumors by using proton magnetic resonance spectroscopy.** *Nature Med* 1996;2:323–325
29. Negendank WG, Sauter R, Brown TR, et al. **Proton magnetic resonance spectroscopy in patients with glial tumors: a multicenter study.** *J Neurosurg* 1996;84:449–458
30. Poptani H, Gupta RK, Roy R, et al. **Characterization of intracranial mass lesions with in vivo proton MR spectroscopy.** *AJNR Am J Neuroradiol* 1995;16:1593–1603
31. Michaelis T, Merboldt KD, Bruhn H, et al. **Absolute concentrations of metabolites in the adult human brain in vivo: quantification of localized proton MR spectra.** *Radiology* 1993;187: 219–227
32. Fulham MJ, Bizzi A, Dietz MJ, et al. **Mapping of brain tumor metabolites with proton MR spectroscopic imaging: clinical relevance.** *Radiology* 1992;185:675–686
33. Langen K-J, Coenen HH, Roosen N, et al. **SPECT studies of brain tumors with L-3-[^{123}I]Iodo-α-methyl tyrosine: comparison with PET, ^{124}IMT and first clinical results.** *J Nucl Med* 1990;31:281–286
34. Kuwert T, Morgenroth C, Woesler B, et al. **Uptake of iodine-123-alpha-methyltyrosine by gliomas and non-neoplastic brain lesions.** *Eur J Nucl Med* 1996;23:1345–1353
35. Grosu AL, Weber W, Feldmann HJ, et al. **First experience with I-123-alpha-methyl-tyrosine SPECT in the 3-D radiation treatment planning of brain gliomas.** *Int J Radiat Oncol Biol Phys* 2000;47:517–526